J|A|C|S
COMMUNICATIONS

Published on Web 01/05/2006

Enhanced Magnetic Properties of Self-Assembled FePt Nanoparticles with MnO Shell

Shishou Kang,* G. X. Miao, S. Shi, Z. Jia, David E. Nikles, and J. W. Harrell

Center for Materials for Information Technology, The University of Alabama, Tuscaloosa, Alabama 35487-0209

Received October 27, 2005; E-mail: skang@mint.ua.edu

The controlled fabrication of very small structures at scales beyond the limits of lithographic techniques is a technological goal of great practical and fundamental interest. Magnetic nanoparticles are now receiving considerable attention because of their wide range of applications, such as the immobilization of proteins and enzymes,[1] bioseparation,[2] immunoassays,[3] drug delivery,[4] and biosensors.[5] Nanoparticles of ferromagnetic materials are of importance because of their reduced sizes that can support only single magnetic domains. The recent synthesis of arrays of 4 nm diameter FePt nanoparticles with an extremely narrow size distribution has promoted a significant research effort in this area, due to their potential technological application as recording media.[6] To realize the full potential of FePt nanoparticle arrays as a recording medium, high-temperature annealing (~600 °C) is required to form the $L1_0$ phase and enhance the thermal stabilities.[6] However, current postsynthesis annealing techniques lead to poor control over the spatial arrangement of nanoparticles through extensive particle aggregation since the organic coatings usually start to decompose at ~350 °C.[7] Recently, Zeng et al. have developed a route to make bimagnetic core/shell FePt/Fe_3O_4 nanoparticles.[8] Although these bimagnetic core/shell nanoparticles have large energy product, they are not suitable for magnetic media since the particles are strongly exchange coupled, which will increase the media noise.[9] Also, there have been efforts to make magnetic nanoparticles with a Ag or Au shell; however, recent experiments reveal that Au/Ag promotes the sintering as well as lowering the ordering temperature of the FePt nanoparticles.[10] To prevent the coalescence for practical applications, a chemically stable and rigid nonmagnetic metallic−oxide shell might be a good candidate for FePt nanoparticles. MnO is well-known as an anti-ferromagnetic (AFM) material with a melting point above 1600 °C. However, the Néel temperature of MnO is only 122 K, and it should be a nonmagnetic material at room temperature.[11] In this report, we demonstrate that 3.5 nm FePt nanoparticles with tunable size and shape of the MnO shell can be synthesized by varying the ratio of the precursors and the stabilizers. The magnetic moment, coercivity, and blocking temperature of FePt nanoparticles were strongly enhanced with the MnO shell. More dramatically, we show that, by coating a MnO shell, the agglomeration of the FePt nanoparticles can be significantly decreased during the heat treatment.

A general procedure to synthesize the MnO shell is described in the Supporting Information. The size and shape of the MnO shell could be tuned by varying the ratio of the precursors and the stabilizers. Figure 1 shows representative TEM images of a cubic-like FePt/MnO core/shell nanoparticle. Although there is a very small amount of FePt nanoparticles that were not coated by a MnO shell, each larger particle in Figure 1 clearly shows a small dark FePt core with a light MnO shell, although there are some dark MnO shells due to the different crystalline orientation. The uncoated FePt nanoparticles can be easily separated by a size selection procedure.[6,12] The electron diffraction (ED) pattern in Figure 1 shows a 4-fold symmetry, indicating a shape-induced texture in these nanoparticles.[13]

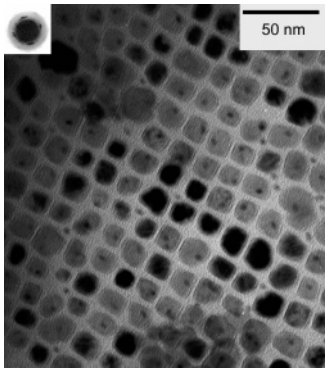

Figure 1. TEM image and ED pattern of FePt nanoparticles with a thick cube-like MnO shell.

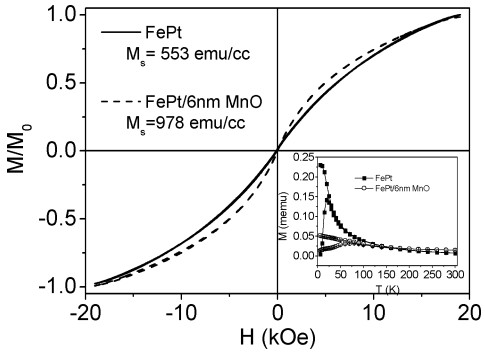

Figure 2. Room temperature hysteresis loops of FePt and FePt/MnO nanoparticles. Inset: ZFC−FC curves of FePt and FePt/MnO nanoparticles, recorded under 50 Oe field.

The room temperature hysteresis loops of as-made FePt and FePt/MnO nanoparticles are shown in Figure 2. It is clear that both MnO coated and uncoated FePt nanoparticles exhibit a superparamagnetic behavior. If we assume the magnetic volume is the same for MnO coated and uncoated FePt nanoparticles, the particle moment can be fitted based on the Langevin function (see the Supporting Information). Fitted results show that M_s values for MnO coated and uncoated FePt nanoparticles are 978 and 553 emu/cc, respectively. The enhanced M_s of MnO coated FePt nanoparticles is due to the interaction between the surface spin of FePt particle and MnO, which could significantly reduce the thickness of magnetic dead layer and/or canted spin layer (due to broken symmetry at the surface) of FePt particles.[7,14] The inset of Figure 2 shows the field-cooled (FC) and zero-field-cooled (ZFC) magnetization. The blocking temperature is increased from 25 to ~75 K for FePt nanoparticles after coating with a MnO shell. It is obvious that, through the pinning of AFM MnO, the FePt nanoparticles are more stable against thermal fluctuations.[15] The pinning of AFM MnO

10.1021/ja057343n CCC: $33.50

can also shift the low-temperature hysteresis loop and increase the saturation field of FePt nanoparticles (see Supporting Information, Figure S3).

As mentioned above, the distinct advantage for making the MnO shell is to prevent the agglomeration of FePt nanoparticles during the high-temperature annealing process, which is required to form the $L1_0$ phase of the FePt nanoparticle. Figure S4 shows the XRD patterns for high-temperature annealed FePt nanoparticles with and without a MnO shell (see Supporting Information). To clearly see the evolution of the superlattice peaks of the $L1_0$ FePt particles, the average thickness of the MnO shell is only about 0.5 nm (estimated from the atomic ratio of the FePt and MnO based on the EDX spectrum). It is obvious that the FePt for both cases is transformed to the $L1_0$ phase, as indicated by the superlattice peaks of the chemically ordered FePt particles. However, the peaks for the pure FePt nanoparticles are much more narrow than the particles with the MnO shell. Scherrer's analysis indicates there is significant aggregation of the FePt particles without the MnO shell during annealing.

The room temperature hysteresis loops and remanence curves reveal that the FePt nanoparticles without the MnO shell have a large coercivity around 14 kOe, while FePt nanoparticles with a MnO shell shows a sheared loop with a small coercivity about 3 kOe (see Supporting Information, Figure S5). For FePt nanoparticles, it is well-known that the coercivity strongly depends on the degree of chemical ordering as well as particle size. With decreasing particle size, thermal agitation will significantly decrease the coercivity. Furthermore, the hysteresis loop of the annealed FePt nanoparticles with the MnO shell shows a soft component, and the remanence coercivity is 3 times larger than the ordinary coercivity. These facts suggest a large anisotropy distribution in the annealed FePt nanoparticles with the MnO shell.[16] Yu et al. have demonstrated that there exists a wide distribution of atomic composition of individual FePt nanoparticles. They showed that when FePt nanoparticles aggregate and sinter during high-temperature annealing, the composition of the aggregates is much more equiatomic than the individual nanoparticles.[17a] For FePt nanoparticles with a MnO shell, there may be a small fraction of particles with composition far from the average stoichiometry and thus may be difficult to chemically order. These particles would give a soft component shown in the hysteresis loop, as seen in Figure S5b, and contribute to a large anisotropy distribution. Another reason for the low coercivity may be related to the effect of the MnO shell on the mobility of the surface atoms of FePt. Also, the size effect on chemical ordering must be considered.[17b] It has been shown that under the same annealing conditions small isolated particles are more difficult to order than large aggregates.[17]

To determine the intrinsic (short time) remanent coercivity, H_0, and thermal stability factor, K_uV/kT, of the annealed FePt nanoparticles, the remanent coercivity was measured as a function of time.[18] Figure 3 shows the time dependence of remanence coercivity for annealed FePt nanoparticles with and without a MnO shell. A fit to the Sharrock formula gave $H_0 \sim 16$ kOe for both coated and uncoated FePt nanoparticles. The K_uV/k_BT values obtained by fitting are 598 and 98, respectively. K_uV/k_BT of uncoated FePt nanoparticles is 6 times larger than that of FePt nanoparticles with a MnO shell, indicating a significant agglomeration of the uncoated FePt nanoparticles during annealing. Although the Sharrock formula may not accurately apply for highly sintered particles, the magnetic results are consistent with the XRD measurement above.

Recently, we have demonstrated that the easy axis of directly synthesized and partially chemically ordered FePt nanoparticles can be aligned.[19] However, the coercivity of the as-made partially ordered FePt nanoparticles is too small for high-density recording. If these particles can be coated with a MnO shell, we can first align the core/shell particles and then furnace anneal them in order to increase the coercivity for media applications, while hopefully maintaining easy axis alignment without sintering. This further investigation is underway.

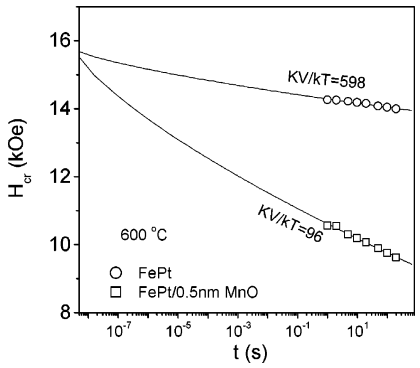

Figure 3. The time dependence of remanence coercivity for pure FePt nanoparticles (opened circle) and FePt/MnO core/shell nanoparticles (opened square). Both samples are annealed at 600 °C for 30 min. Solid lines are fitted based on the Sharrock formula in ref 18.

Acknowledgment. This work was supported by the NSF Materials Research Science and Engineering Center Award No. DMR-0213985.

Supporting Information Available: Full synthetic details. This material is available free of charge via the Internet at http://pubs.acs.org.

References

(1) Chen, D.-H.; Liao, M.-H. *J. Mol. Catal. B Enzymol.* **2002**, *16*, 283.
(2) (a) Rooth, S. *J. Magn. Magn. Mater*. **1993**, *122*, 329. (b) Sonti, S. V.; Bose, A. *J. Colloid Interface Sci.* **1995**, *170*, 575.
(3) Sauzedde, F.; Elaissari, A.; Pichat, C. *Macromol. Symp*. **2000**, *151*, 617.
(4) Rudge, R. S.; Kurtz, T. L.; Vessely, C. R.; Catterall, L. G.; Williamson, D. L. *Biomaterials* **2000**, *21*, 1411.
(5) Varlan, A. R.; Sansen, W.; Van, L. A.; Hendrickx, M. *Biosens. Bioelectron.* **1996**, *11*, 443.
(6) Sun, S.; Murray, C. B.; Weller, D.; Folks, L.; Moser, A. *Science* **2000**, *287*, 1989.
(7) Wu, X. W.; Liu, C.; Li, L.; Jones, P.; Chantrell, R. W.; Weller, D. *J. Appl. Phys*. **2004**, *95*, 6810.
(8) Zeng, H.; Li, J.; Wang, Z. L.; Liu, J. P.; Sun, S. *Nano Lett*. **2004**, *4*, 187.
(9) Weller, D.; Moser, A.; Folks, L.; Best, M. E.; Lee, W.; Toney, M. F.; Schwickert, M.; Thiele, J.-U.; Doerner, M. F. *IEEE Trans. Magn*. **2000**, *36*, 10.
(10) Harrell, J. W.; Nikles, D. E.; Kang, S.; Sun, X.; Jia, Z.; Shi, S.; Lawson, J.; Thompson, G. B.; Srivastava, C.; Seetala, N. V. *Scripta Mater*. **2005**, *53*, 411.
(11) (a) Ahmad, T.; Ramanujachary, K. V.; Lofland, S. E.; Ganguli, A. K. *J. Mater. Chem*. **2004**, *14*, 3406. (b) Masala, O.; Seshadri, R. *J. Am. Chem. Soc.* **2005**, *127*, 9354.
(12) Sun, S.; Anders, S.; Thomson, T.; Baglin, J. E. E.; Toney, M. F.; Hamann, H. F.; Murray, C. B.; Terris, B. D. *J. Phys. Chem. B* **2003**, *107*, 5419.
(13) Zeng, H.; Rice, P. M.; Wang, S. X.; Sun, S. *J. Am. Chem. Soc.* **2004**, *126*, 11458.
(14) Thomson, T.; Toney, M. F.; Raoux, S.; Lee, S. L.; Sun, S.; Murray, C. B.; Terris, B. D. *J. Appl. Phys.* **2004**, *96*, 1197.
(15) Skumryev, V.; Stoyanov, S.; Zhang, Y.; Hadjipanayis, G.; Givord, D.; Nogues, J. *Nature* **2003**, *423*, 850.
(16) Wang, S.; Kang, S.; Harrell, J. W.; Chantrell, R. W. *Phys. Rev. B* **2003**, *68*, 104413.
(17) (a) Yu, A.; Mizuno, M.; Sasaki, Y.; Kondo, H. *Appl. Phys. Lett*. **2004**, *85*, 6242. (b) Miyazaki, T.; Kitakami, O.; Okamoto, S.; Shimada, Y.; Akase, Z.; Murakami, Y.; Shindo, D.; Takahashi, Y.; Hono, K. *Phys. Rev. B* **2005**, *72*, 144419.
(18) Sharrock, M. P.; McKinney, J. T. *IEEE Trans. Magn.* **1981**, *17*, 3030.
(19) Kang, S.; Jia, Z.; Shi, S.; Nikles, D. E.; Harrell, J. W. *Appl. Phys. Lett.* **2005**, *86*, 062503.

JA057343N